Bulletin of Pharmaceutical Research 2015;5(2):70-80
An Official Publication of Association of Pharmacy Professionals
ISSN: 2249-6041 (Print); ISSN: 2249-9245 (Online)

RESEARCH PAPER

QSAR STUDIES INVOLVING 2D, 3D QSAR AND PHARMACOPHORE MAPPING STUDIES ON ARYLSULFONYL IMIDAZOLIDINONE DERIVATIVES AS ANTICANCER AGENTS

Shivangi Agarwal[1], Vikash K. Mishra[1], Mitali Mishra[1], Shivani Singh[2], Vivek Kumar[3], Varsha Kashaw[4] and Sushil K. Kashaw[1]*

[1]Department of Pharmaceutical Sciences, Dr. H.S. Gour Central University, Sagar-470 003, Madhya Pradesh, India
[2]Department of Pharmacognosy and Phytochemistry, Jamia Hamdard University, Hamdard Nagar, New Delhi-110 062, India
[3]Department of Pharmaceutical Chemistry, National Institute of Pharmaceutical Education and Research, Mohali, Chandigarh-160 062, India
[4]Department of Pharmaceutical Chemistry, Sagar Institute of Pharmaceutical Sciences, Sagar-470 228, Madhya Pradesh, India.

**E-mail*: sushilkashaw@gmail.com
Tel.: +91 9425655720.

Received: July 9, 2015 / Revised: Aug 21, 2015 / Accepted: Aug 22, 2015

QSAR analysis including 2D QSAR, 3D QSAR and pharmacophore mapping studies have been performed on a series of arylsulfonylimidazolidinone derivatives to explore the physico-chemical properties and basic pharmacophore responsible for anti-cancer activity. The 2D-QSAR studies were carried out using the partial least squares (PLS) method coupled with stepwise variable selection, with $r^2 = 0.7106$ and $q^2 = 0.5176$; the 3D-QSAR studies were performed using stepwise variable selection k-nearest-neighbor molecular field analysis (kNNMF) approach; with cross-validated correlation coefficient (q^2) of 0.5909. Pharmacophore mapping resulted in highly predictive pharmacophore based 3D-QSAR model with five point hypotheses (AADHR.18) with two acceptor atom, one donor group, one hydrophobic group and one aromatic ring as pharmacophore features. This is denoted as A2A3D5R10H7. Research indicated that alignment-independent descriptors, steric field and electrostatic field descriptors were significantly correlating with anticancer activity of arylsulfonylimidazolidinone derivatives.

Key words: QSAR, Pharmacophore mapping, Arylsulfonylimidazolidinone, Anticancer activity, kNNMF.

INTRODUCTION

Much of the general public sees cancer as a modern day plague that results in high morbidity (Green and Evan, 2002). Cancer cells rapidly acquire resistance against numerous cytotoxic drugs or are even intrinsically resistant. Despite over 50 years of research, it is still debated, how cancer cells generate complex resistance phenotypes against a multitude of drugs much more rapidly than predicted by conventional mutation, and how cancer cells generate such resistance with the very same genes they just inherited from normal, drug sensitive precursor cells (Duesberg *et al* 2007). The occurrence of localized changes in chromatin structure at transcriptional start sites has been well appreciated; however, it is now emerging that the alterations are genome wide.

Indeed, early studies pointed to an overall decrease in the 5-methylcytosine content of cancer genomes (Jones and Baylin, 2007). Use of computational techniques in drug discovery and development process is rapidly gaining in popularity, implementation and appreciation. These methods are expected to limit and focus chemical synthesis and biological testing and thereby greatly decrease traditional resource requirements (Kapetanovic, 2008). Drugs are essential for the prevention and treatment of disease. Human life is constantly threatened by many diseases such as cancer. Therefore, ideal drugs are always in great demand. To meet the challenges of ideal drugs, an efficient method of drug development is demanding (Mandal *et al* 2009). Having emerged as a quantitative structure activity relationship (QSAR) analysis in the early 1960s, the concept of CADD has evolved very quickly, especially in the recent decade as an unprecedented development of structural biology and computer capabilities. CADD technologies including molecular modeling and simulation have become promising in drug discovery (Tang *et al* 2006; Bansal *et al* 2011; Kumar, 2011; Sharma *et al* 2011; Jain *et al* 2013). Quantitative structure activity relationship (QSAR) research field has been widely developed, from its very first beginnings when, in 1865, Crum-Brown and Fraser postulated a relationship between any physiological activity and the corresponding chemical structure (Saliner and Girones, 2005). The key goal of computer-aided molecular design methods in modern medicinal chemistry is to reduce the overall cost associated with the discovery and development of a new drug, by identifying the most promising candidates to focus on the experimental efforts (Langer and Wolber, 2004). In drug discovery, the chemoinformatics techniques such as virtual screening, pharmacophore modeling, quantitative structure-activity relationship (QSAR), data mining, etc. are of great significance, being considerably precise as well as saving time and cost. One of the several ways is to develop a 3D-pharmacophoremodel and utilize it in the virtual screening of available databases, which seems to be more significant and time saving (Ambure *et al* 2014). A pharmacophore (pharmacophore model, pharmacophoric pattern) can be considered as the ensemble of steric and electrostatic features of different compounds which are necessary to ensure optimal supramolecular interactions with a specific biological target structure and to trigger or to block its biological response (Langer and Wolber, 2004). 3D pharmacophore based techniques have become one of the most important approaches for the fast and accurate virtual screening of databases with millions of compounds. The success of 3D pharmacophore is largely based on their intuitive interpretation and creation (Seidel *et al* 2010). The pharmacophore detection module is able to: (i) align multiple flexible ligands in a deterministic manner without exhaustive enumeration of the conformational space, (ii) detect subsets of input ligands that may bind to different binding sites or have different binding modes, (iii) address cases where the input ligands have different affinities by defining weighted pharmacophore based on the number of ligands that share them, and (iv) automatically select the most appropriate pharmacophore candidates for virtual screening (Dror *et al* 2009). In present investigation, QSAR analysis including 2D QSAR, 3D QSAR and pharmacophore mapping studies were performed on a series of arylsulfonylimidazolidinone derivatives to explore the physico-chemical properties and basic pharmacophore responsible for anti-cancer activity.

MATERIALS AND METHODS

A set of 32 molecules of arylsulfonyl imidazolidinone derivatives reported by (Park Choo *et al* 2003) was subjected to the 2D, 3D QSAR analysis and pharmacophore mapping for their anticancer activity. All QSAR studies were performed in V-Life MDS software Version 3.5 and the pharmacophore mapping was performed by Schrodinger Maestro 9.5. (Phase 2013; Maestro, 2013). The biological activity of the compounds was reported as IC_{50} values (nm) and converted to pIC_{50} (log $1/IC_{50}$) values. The structures of all 32 compounds along with their biological activity values are included in **Table 1**.

Processing of molecules

The set of molecules considered in this study was sketched and optimized by MMFF method for 2D, 3D QSAR method. For pharmacophore mapping, the molecules were geometrically refined using LigPrep module implemented in the "Maestro suite" program (version 9.5) (Maestro, 2012). After the sketching of all molecules, cleaning and conformational search was performed in "develop pharmacophore" module of PHASE.

The conformations were generated by the Monte Carlo (MCMM) method as implemented in

MacroModel version 9.5 using a maximum of 1000 steps with a distance-dependent dielectric solvent model and an OPLS-2005 force field. These conformers were employed for the development of pharmacophore model (Mehta *et al* 2012).

Table 1. Structure of the compounds in the series along with their biological activity

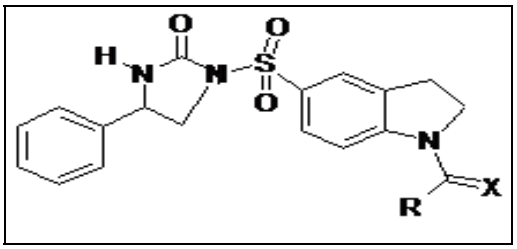

Molecule	X	R	$_{P}IC_{50}(\mu M)$
S1	O	-$NHCH_2CH_3$	0.107
S2	O	-$NHCH(CH_3)_2$	0.770
S3	O	-NHC_6H_{11}	2.254
S4	O	-NHC_6H_5	0.347
S5	O	-NHC6H4(4-NH2)	0.207
S6	S	-$NHCH_2CH_3$	0.013
S7	S	$NHCH_2CH_2CH_3$	0.299
S8	S	$NHCH_2CH_2CH_2CH_3$	-0.09
S9	S	-NHC_6H_5	0.664
S10	O	$NHC_6H_4(2\text{-}OCH_3)$	0.537
S11	O	$NHC_6H_4(4\text{-}CH_3)$	0.198
S12	O	C_6H_5	0.048
S13	O	$C_6H_4(2\text{-}OH)$	-0.113
S14	O	$C_6H_4(4\text{-}OEt)$	0.613
S15	O	$C_6H_4(4\text{-}Cl)$	-0.062
S16	O	$C_6H_4(2\text{-}NO_2)$	-0.624
S17	O	$C_6H_4(2\text{-}CN)$	-0.491
S18	O	$C_6H_4(4\text{-}NH_2)$	0.737
S19	O	$C_6H_4(3\text{-}Cl)$	-0.387
S20	O	$C_6H_4(3\text{-}F)$	0.205
S21	O	$C_6H_3(2,4\text{-}F)$	-0.577
S22	O	$C_6H_4(3\text{-}OCF_3)$	-0.701
S23	O	$C_6H_4(4\text{-}OCF_3)$	-0.102
S24	O	$NHCH_2CH_2CH_3$	-0.053
S25	O	$NHC_6H_4(4\text{-}OCH_3)$	0.431
S26	S	$NHCH_3$	1.158
S27	S	$NHC_6H_4(4\text{-}OCH_3)$	0.269
S28	O	$C_6H_4(4\text{-}OCH_3)$	0.292
S29	O	$C_6H_3(3,4\text{-}OCH_3)$	0.201
S30	O	$C_6H_4(4\text{-}F)$	-0.360
S31	O	$C_6H_3(3,5\text{-}Cl)$	-0.187
S32	O	$C_6H_4(3\text{-}CF_3)$	-0.659

2D QSAR

All the compounds for 2D QSAR were subjected to energy minimization by MMFF (Molecular mechanics force field method). Various 2D descriptors like topological, physicochemical, alignment-independent descriptors were calculated after which by invariable column was removed and the training and test set was selected by manual selection method. The model for the 2D-QSAR study was generated using PLS with forward backward as the variable selection method.

3D QSAR

For studies, the molecules were converted from 2D to 3D structures, optimized by MMFF (Molecular mechanics force field method) and then were aligned using template based

alignment method by taking most active molecule B3 (**Figure 1**) as the reference molecule and basic moiety (**Figure 2**) as the template. The alignment is shown in **Figure 3**. The QSAR model was built by kNN method using forward-backward as variable selection method. It examines the steric fields and the electrostatic fields. 3D-QSAR refers to the application of force field calculations requiring three dimensional structures, e.g. based on protein crystallography or molecule superimposition (Ibezim *et al* 2009).

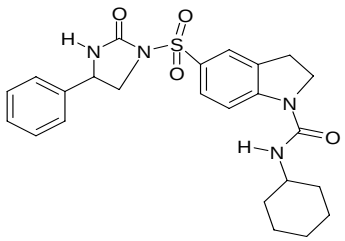

Fig. 1. Reference molecule (B3) used for alignment by template based alignment

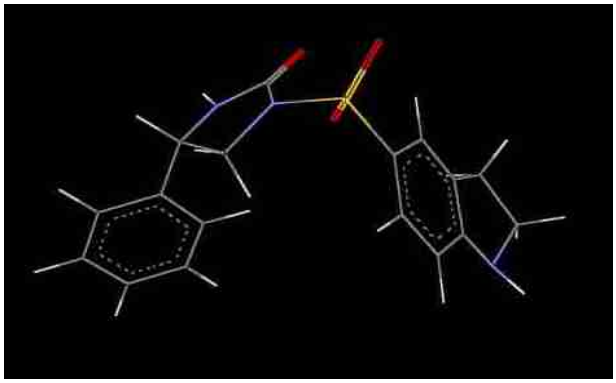

Fig. 2. Basic moiety as a template for alignment

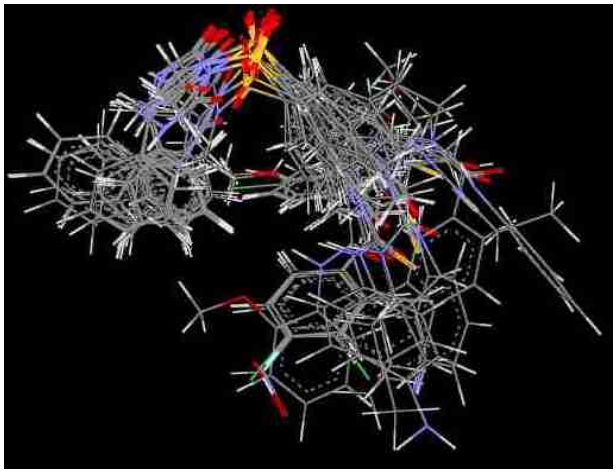

Fig. 3. 3D view of aligned molecules

Pharmacophore mapping

Phase methodology

Pharmacophore modeling was carried out using PHASE: a module of Schrödinger's software program 'MAESTRO' [9.5] (Mehta *et al* 2012; Phase, 2013). This pharmacophore was used as alignment rule in order to develop a 3D-QSAR model (Dixon *et al* 2006). Phase provides the option of doing QSAR with the selected pharmacophore hypothesis (Rathi Suganya *et al* 2011).

Preparing ligands

The chemical structures of all the compounds were drawn in maestro and geometrically refined using LigPrep module. LigPrep was used to attach hydrogen, converts 2D structures to 3D, generates stereoisomer, and, optionally, neutralizes charged structures or determines the most probable ionization state at user defined pH. All the structures were ionized at neutral pH 7. The conformations were generated by the Monte Carlo (MCMM) method as implemented in Macro Model version 9.6 using a maximum of 100 steps with a distance-dependent dielectric solvent model and an OPLS-2005 force field.

Pharmacophore hypothesis generation

The next step in developing a pharmacophore model is to use a set of pharmacophore features to create pharmacophore sites (site points) for all the ligands. Once a feature has been mapped to a specific location in a conformation, it is referred to as a pharmacophore site. Common pharmacophoric features were then identified from a set of variants-a set of feature types that define a possible pharmacophore. In the next step, common pharmacophore hypothesis were examined using a scoring function i.e. survival scores of actives and inactives (Mehta *et al* 2012). The hypotheses were scored using default parameters for site, vector, volume, selectivity, number of matches, and energy terms.

The regression analysis was performed by constructing a series of models with an increasing number of PLS factors. Pharmacophore-based 3D-QSAR models were generated for the hypotheses (Kaur *et al* 2012).

RESULTS AND DISCUSSION

2D QSAR

The best QSAR model was selected among the various models generated by PLS (Partial Least Square analysis). The 2D QSAR equation and the statistical parameters generated are shown in the **Table 2**.

The QSAR model shows r^2= 0.7106 and standard error of 0.3512 which indicates the accuracy of

the statistical fit. The stability of model judged by leave-one-out procedure is fairly good (q^2 =0.5176) suggesting that the models will be useful for meaningful predictions. The descriptors contributing to the biological activity as generated are T_2_2_4, Polarizability AHC and smr. The correlation matrix given in **Table 3**. In the correlation matrix, the values less than 0.6 indicate the absence of multi co-linearities in the model. **Figure 4** gives a pictorial representation of different 2D parameters and their contributions towards antitubercular activity. The 2D parameters contributed to the biological activity can be defined as below.

Table 2. Statistical results of 2D QSAR equation generated by PLS method

Equation	pIC_{50} = - 0.2172 T_2_2_4 -0.1950 Polarizability AHC + 0.0565 smr+2.0294
Statistics	n = 25, Degree of freedom = 22, F test = 27.0052, r^2 = 0.7106, q^2 = 0.5176, pred_r^2 = -0.0890, r^2 se = 0.3512, q^2 se = 0.4534, pred_r^2se= 0.4986

Table 3. Correlation Matrix for the descriptors contributing to the 2D QSAR model

	smr	Polarizibility AHC	T_2_2_4	Score
smr	1	0.406	0.295	3
Polarizibility AHC	0.406	1	-0.366	3
T_2_2_4	0.295	-0.366	1	3
T_N_O_6	0.282	0.046	0.417	3

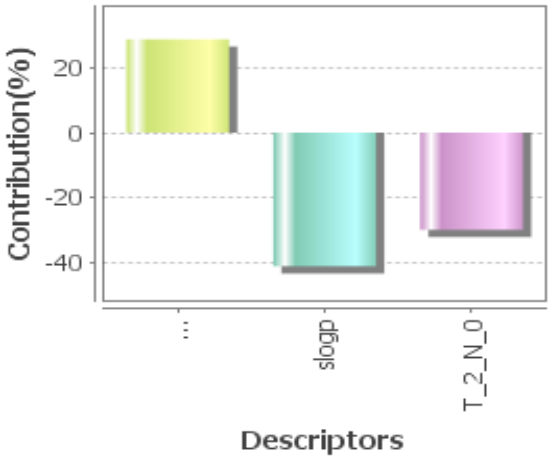

Fig. 4. Contribution chart of selected 2D descriptors for anticancer activity

Polarizability AHC

This descriptor evaluates molecular polarizability using sum of atomic polarizability using the atomic hybrid component (AHC).

smr

This descriptor evaluates molecular refractivity (including implicit hydrogen) which also measure of molecular size. This property is an atomic contribution model that assumes the correct protonation state.

T_2_2_4

This is the count of number of double bounded atoms (i.e. any double bonded atom, T_2) separated from any other double bonded atom by 4 bonds in a molecule. Uni-column statistics as shown in **Table 4** for training and test set were generated to check correctness of selection criteria for training and test set molecules. Higher standard deviation in training set indicates wide distribution of activity of molecules as compared to test set molecules.

Table 4. Uni-Column statistics for training set and test set

Set	Column name	Average	Max	Min	Std Dev	Sum
Training	pIC_{50}	0.2166	2.2540	-0.7010	0.6250	5.4160
Test	pIC_{50}	0.0154	0.6130	-0.6590	0.4225	0.1080

Figure 5 showed the graph plotted between actual and predicted biological activity. Training set (points in red) as well as test set (points in blue) are well closed to regression line and also the training set are encircling the test set showing good predictive ability of the model. The predicted activity values for the compounds in the training set and test set, along with their corresponding observed activity values, are given in **Table 5**.

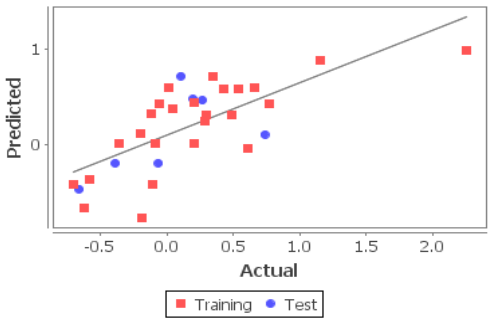

Fig. 5. Fitness plot between observed and predicted biological activities of training (blue spot) and test (red spot) molecules of 2D model.

3D QSAR

3D-QSAR was used to optimize the steric and electrostatic requirement. 3D data points were generated that contributed to k nearest neighbor molecular field analysis (kNN-MFA) 3D-QSAR model.

This is followed by generation of a common rectangular grid around the molecules. The steric interaction energies are computed at the lattice points of the grid using a methyl probe of charge +1.

The data points generated by 3D-QSAR are shown in **Figure 6.**

Table 5. Observed and predicted activity of training set and test set with their residuals of 2D QSAR

Comp no.	pIC_{50} (nm)	Prediction (μm)	Residual
*1	0.107	0.549014	-0.44201
2	0.770	0.519922	0.250078
3	2.254	1.97573	0.27827
4	0.347	0.699635	-0.35264
5	0.207	0.725389	-0.51839
6	0.013	0.452699	-0.4397
*7	0.299	0.413884	-0.11488
*8	-0.090	0.370857	-0.46086
9	0.664	0.673707	-0.00971
10	0.537	0.406811	0.130189
*11	0.198	0.673055	-0.47506
12	0.048	0.249832	-0.20183
13	-0.113	-0.11675	0.00375
*14	0.613	-0.039409	0.652409
15	-0.062	-0.037124	-0.02488
16	-0.624	-0.66131	0.03731
17	0.491	-0.007979	0.498979
18	0.737	0.278722	0.458278
19	-0.387	-0.037124	-0.34988
20	0.205	-0.016227	0.221227
21	-0.577	0.298364	-0.87536
22	-0.701	-0.190972	-0.51003
23	-0.102	-0.190972	0.088972
24	-0.053	0.521165	-0.57417
25	0.431	0.406811	0.024189
26	1.158	0.486803	0.671197
27	0.269	0.342933	-0.07393
28	0.292	-0.030022	0.322022
29	-0.201	-0.36707	0.16607
30	-0.360	-0.016227	-0.34377
*31	-0.187		
*32	-0.659		

*Test compound

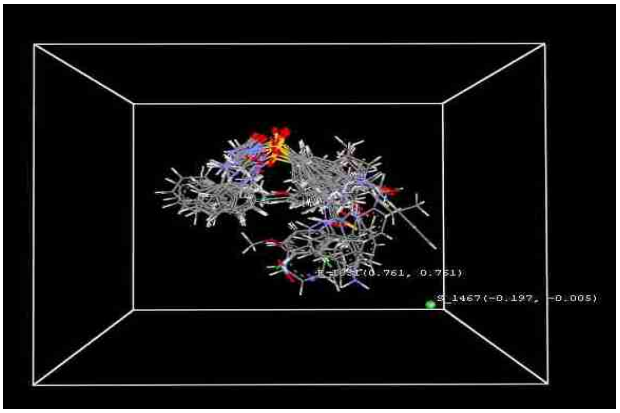

Fig. 6. Relative positions of the steric and electrostatic fields around aligned molecules

The best model generated with kNN MFA method showed a q^2 as 0.5909 as shown in **Table 6**. The predicted activity values for the compounds in the training set and test set, along with their corresponding actual activity values, are given in **Table 7**.

Table 6. Statistical results of 3D QSAR model generated by SW kNN MFA method

Model summary	
Training Set Size	= 25
Test Set Size	= 7
k Nearest Neighbor	= 2
n	= 25
Degree of freedom	= 22
q^2	= 0.5909
q^2_se	= 0.2095
Pred_r^2	= -0.5099
pred_r^2se	= 0.4684
E_1031	(0.7611,0.7615)
S_1467	(-0.1972, 0.0050)

Table 7. Actual and predicted activity of training set and test set with their residuals of 3D QSAR

Comp no.	**PIC_{50} (nm)**	**Prediction (nm)**	**Residual**
*1	0.107	0.258057	-0.15106
2	0.770	-0.153712	0.923712
3	2.254	-0.922569	3.176569
4	0.347	0.437864	-0.09086
5	0.207	0.513135	-0.30614
6	0.013	-0.101923	0.114923
*7	0.299	0.921297	-0.6223
8	-0.090	-0.157614	0.067614
9	0.664	0.274351	0.389649
10	0.537	0.455364	0.081636
11	0.198	-0.049521	0.247521
12	0.048	0.216786	-0.16879
13	-0.113	-0.036712	-0.07629
14	0.613	0.415073	0.197927
15	-0.062	-0.092873	0.030873
16	-0.624	-0.679782	0.055782
*17	0.491	0.110385	0.380615
18	0.737	0.574535	0.162465
19	-0.387	-0.124462	-0.26254
20	0.205	-0.221524	0.426524
*21	-0.577	0.246325	-0.82333
22	-0.701	-0.64146	-0.05954
*23	-0.102	-0.146464	0.044464
*24	-0.053	0.2023	-0.2553
25	0.431	0.449473	-0.01847
26	1.158	1.35791	-0.19991
*27	0.269	0.406881	-0.13788
28	0.292	0.52064	-0.22864
29	-0.201	-0.101012	-0.09999
30	-0.360	0.412482	-0.77248
31	-0.187	-0.227113	0.040113
32	6.333	0.66132	5.67168

**Test set*

Figure 7 showed the graph plotted between actual and predicted biological activity. Training set (points in red) as well as test set (points in blue) are well closed to regression line and showing good predictive ability of the model. The ranges of data point values were based on the variation of the field values at the chosen points using the most active molecule and its nearest neighbor set. Points generated in SA kNN–MFA 3D-QSAR model are S_1467 (-0.1972, 0.0050), E_1031 (0.7611, 0.7615) i.e. steric data points at lattice points 1467 and electrostatic at 1031 respectively.

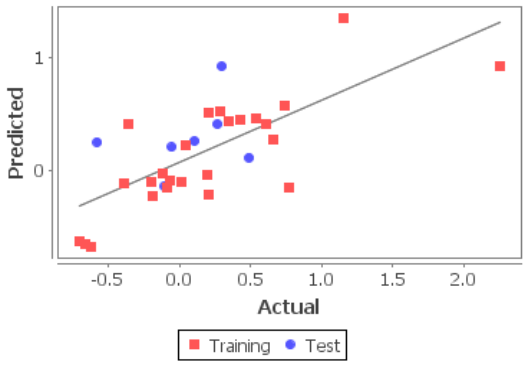

Fig. 7. Fitness plot between observed and predicted activities of the training (blue spot) and test (red spot) molecules of 3D model

Pharmacophore mapping

The pharmacophore mapping studies were performed on the series of arylsulfonyl imidazolidinone derivatives to identify common structural features required for the biological activity. A total of 4 different variant hypotheses were generated upon completion of common pharmacophore identification process. The result of top four hypotheses high gradient score is recorded in **Table 8**.

The top model was found to be associated with the five point hypotheses (AADHR.18) which consist of two acceptor group (A), one donor group (D), one hydrophobic group (H) and one aromatic rings (R). This is denoted as A2A3D5H7R10. The best hypothesis showed the survival score as 3.728.

The common pharmacophoric features are then scored with reference to the volume occupied by training set molecules. The special disposition of the sites showing distance between pharmacophoric sites is shown in **Figure 8**. The pharmacophoric sites mapping over all the molecules of dataset as well as active molecule is shown in **Figure 9** and **Figure 10** respectively.

The pharmacophore hypothesis yielded a 3D-QSAR model with good PLS statistics. Among various PLS factors, PLS factor 4 was selected on the basis of statistical parameters. The training set correlation is characterized by PLS factor 4 (r^2 = 0.94, SD = 0.1861, F = 66.6, stability=0.1067). Results of PLS statistics of 3D QSAR model are shown in **Table 9**.

Table 8. Scoring results of the different hypotheses generated

S. No	ID	Survival	Survival-inactive	Post-hoc	Site	Vector	Volume	Selectivity
1	AHRR.100	3.728	1.136	3.728	0.88	1	0.846	1.752
2	AADHR.18	3.728	1.152	3.728	0.94	1	0.788	1.613
3	AAAHR.3	3.727	1.15	3.727	0.93	1	0.793	1.588
4	ADHRR.53	3.724	1.07	3.725	0.93	1	0.799	1.859

Table 9. Statistical results of generated 3D QSAR model

PLS	SD	r^2	F	Stability	RMSE	Q^2	Pearson-R
1	0.5544	0.3741	12	0.8794	0.3263	-0.5417	0.6026
2	0.3456	0.7689	31.6	0.1369	0.2564	0.0478	0.5226
3	0.263	0.8732	41.3	-0.0392	0.2577	0.0383	0.4744
4	0.1861	0.94	66.6	0.1067	0.3131	-0.4196	0.3526

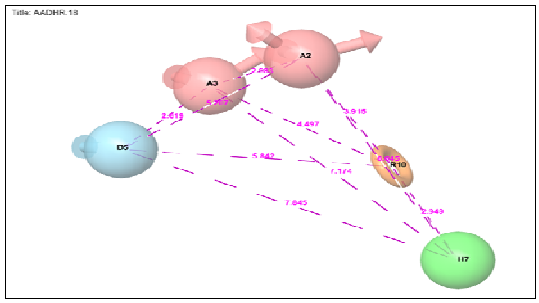

Fig. 8. Selected hypothesis: AADHR.18

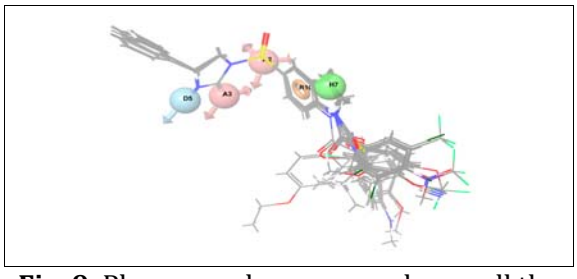

Fig. 9. Pharmacophore mapped over all the molecules of data set

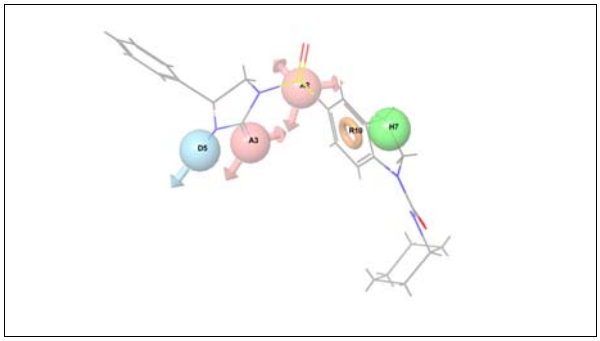

Fig. 10. Pharmacophore mapped over active molecule

The model was selected on the basis of value of r^2. The generated best model was further validated for its external predictability. For model generation and validation, the total molecules were divided into training (22) and test (11) set molecules. The reliability of the model can be judged based on the external prediction. The fitness scores of training and test set molecules are presented in the **Table 10**. The correlation scatter plot between actual and predicted values of biological activity of training and test set is presented in **Figure 11**.

Table 10. Fitness scores of all the training and test set compounds

Ligand name	Pharm set	QSAR set	Fitness
Bs1	Active	test	2.73
Bs2	Active	training	2.84
Bs3	Active	training	3
Bs4		training	2.72
Bs5		training	2.79
Bs6		training	2.8
Bs7		test	2.82
Bs8		training	2.86
Bs9		training	2.83
Bs10		test	2.81
Bs11		test	2.78
Bs12		test	2.6
Bs13		test	2.62
Bs14		training	2.62
Bs15		test	2.59
Bs16	Inactive	training	2.62
Bs17		test	2.56
Bs18	Active	training	2.58
Bs19		training	2.62
Bs20		training	2.58
Bs21	Inactive	training	2.6
Bs22	Inactive	training	2.56
Bs23		training	2.58
Bs24		training	2.77
Bs25		training	2.78
Bs26	Active	training	2.77
Bs27		test	2.66
Bs28		training	2.64
Bs29		training	2.57
Bs30		test	2.58
Bs31		training	2.53
Bs32	Inactive	training	2.54

Contour analysis

Contour plots generated from the best 3D QSAR model are represented as positive and negative activity coefficient of different properties are given in **Figures 12i-iii**. The blue contours represent the regions where the substitution of groups with the particular property may enhance the biological activity whereas red cubes represent the depreciating biological activity.

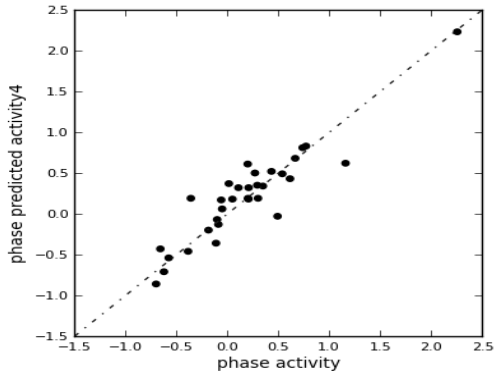

Fig. 11. Correlation scatter plot actual and predicted activity of training and test set molecules

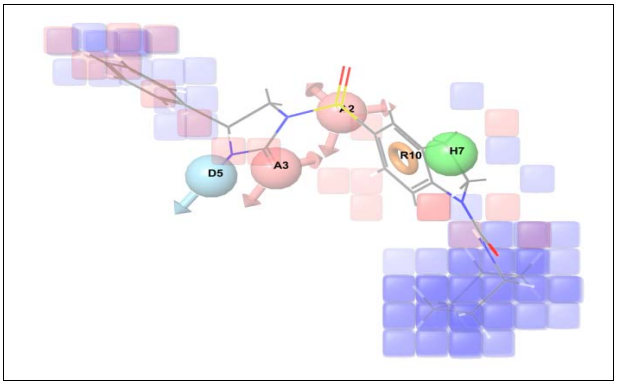

Fig. 12ii. Strereoviews of the hydrophobic/ non-polar properties generated by contour plots by 3D model.

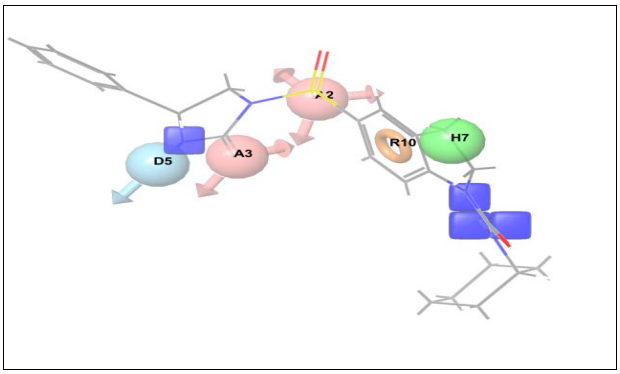

Fig. 12i. Strereoviews of hydrogen bond donor properties generated by contour plots by 3D model.

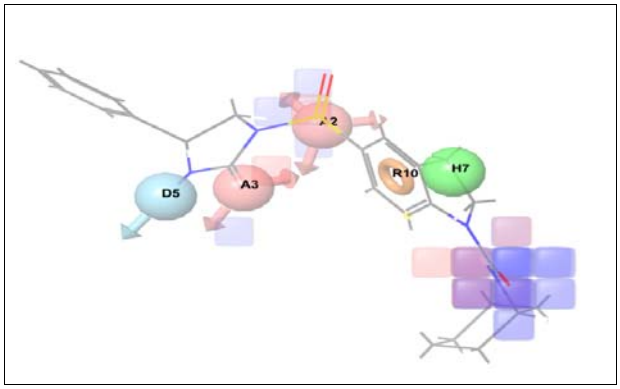

Fig. 12iii. Strereoviews of electron withdrawing properties generated by contour plots by 3D model.

Hydrogen bond donor property contour

As shown in the **Figure 12i**, blue contour around the nitrogen atom of dihydro-indole ring signifies the importance of H-bond donor group at this position.

Hydrophobic property contour

The blue region around both the cyclohexylamide group is in favorable region of positive activity coefficient thereby increasing the activity (**Figure 12ii**). The red region around terminal phenyl group indicates that the particular group is not important for the activity.

Electron withdrawing property contour

The blue contour at carbonyl group attached to the nitrogen of dihydro-indole ring signifies the importance of electron withdrawing group for the activity (**Figure 12iii**).

CONCLUSION

QSAR and pharmacophore mapping studies were performed on arylsulfonylimidazolidinone derivatives for their anticancer activity. 2D QSAR study indicated the requirement of smr which positively contributed to the biological activity and removal of polarizability AHC, T_2_2_4 index which negatively contributed to the biological activity. 3D- QSAR gave information about nature of substituent's like less steric substituent's are required at data points S_1467 (-0.1972, 0.0050) and electrosteric substituent's are required at data point E_1031 (0.7611, 0.7615) for maximum activity. A highly predictive pharmacophore based 3D-QSAR model was generated with five point hypotheses (AADHR.18) with two acceptor atom, one donor group, one hydrophobic group and one aromatic ring as pharmacophore features. This dataset was used to build a QSAR model where the model with best statistics found was with PLS factor 4 with best correlation coefficient (r^2=0.9400), standard deviation (0.1861) and variance ratio (F) (66.6). This model showed correlation coefficient (Q^2) -0.4196 and Pearson R (0.3526) with test set molecules. Contour analysis from our model gave us the following vital information about our core molecule. The

blue contour around the nitrogen atom of dihydro-indole ring signifies the importance of H-bond donor group at this position. The blue region around both the cyclohexylamide group is in favorable region of positive activity coefficient thereby increasing the activity. The red region around terminal phenyl group indicates that the particular group is not important for the activity. The blue contour at carbonyl group attached to the nitrogen of dihydro-indole ring signifies the importance of electron withdrawing group for the activity. Current research work helped us to find important chemical features of arylsulfonylimidazolidinone derivatives which may be utilized further to design new active compounds of cancer.

ACKNOWLEDGEMENT

One of the author wish to acknowledge to the AICTE (All India Council of Technical Education) for granting of the fund for the completion of this project work.

REFERENCES

Ambure P, Kar S, Roy K. Pharmacophore mapping-based virtual screening followed by molecular docking studies in search of potential acetylcholinesterase inhibitors as anti-Alzheimer's agents. *Biosystems* 2014;116:10-20. [DOI: 10.1016/j.biosystems.2013.12.002]

Bansal H, Sharma A, Sharma V, Kumar V. Pharmacophore modeling studies on xanthones as monoamine oxidase-A inhibitors. *Bull. Pharm. Res.* 2011;1(1):15-21.

Dixon SL, Smondyrev AM, Knoll EH, Rao SN, Shaw DE, Friesner RA. PHASE: A new engine for pharmacophore perception, 3D QSAR model development, and 3D database screening: 1. Methodology and preliminary results. *J. Comput. Aided Mol. Des.* 2006;20(10-11):647-71. [DOI: 10.1007/s10822-006-9087-6]

Dror O, Schneidman-Duhovny D, Inbar Y, Nussinov R, Wolfson HJ. A novel approach for efficient pharmacophore-based virtual screening: Method and applications. *J. Chem. Inf. Model.* 2009;49(10):2333-43. [DOI: 10.1021/ci900263d]

Duesberg P, Li R, Sachs R, Fabarius A, Upender MB, Hehlmann R. Cancer drug resistance: the central role of the karyotype. *Drug Resist. Updat.* 2007;10(1-2):51-8. [DOI: 10.1016/j.drup.2007.02.003]

Green DR, Evan GI. A matter of life and death. *Cancer Cell* 2002;1(1):19-30. [DOI: 10.1016/S1535-6108(02)00024-7]

Ibezim EC, Duchowicz PR, Ibezim NE, Mullen LMA, Onyishi IV, Brown SA, Castro EA. Computer-aided linear modeling employing QSAR for drug discovery. *Sci. Res. Assay.* 2009;4(13):1559-64.

Jain J, Bansal SK, Chowdhury P, Sinha R, Tripathi U, Malhotra M. *In silico* pharmacophore validation of anticonvulsant activity of (*E*) (±)-3-menthone derivatives. *Bull. Pharm. Res.* 2013;3(3):146-56.

Jones PA, Baylin SB. The epigenomics of cancer. *Cell* 2007;128(4):683-92. [DOI: 10.1016/j.cell.2007.01.029]

Kapetanovic I.M. Computer-aided drug discovery and development (CADDD): *In silico*-chemico-biological approach. *Chem. Biol. Interact.* 2008;171(2):165-76. [DOI: 10.1016/j.cbi.2006.12.006]

Kaur P, Sharma V, Kumar V. Pharmacophore modelling and 3D-QSAR studies on N^3-phenylpyrazinones as cortico-tropin-releasing factor 1 receptor antagonist. *Int. J. Med. Chem.* 2012(2012):1-13 (Article ID 452325). [DOI: 10.1155/2012/452325]

Kumar V. Topological models for the prediction of tyrosine kinase inhibitory activity of 4-anilinoquinazolines. *Bull. Pharm. Res.* 2011;1(2):53-9.

Langer T, Wolber G. Pharmacophore definition and 3D searches. *Drug Disc. Today: Technol*. 2004;1(3):203-7. [DOI: 10.1016/j.ddtec.2004.11.015]

Maestro, version 9.5, Schrodinger, LLC, New York, 2013.

Mandal S, Moudgil M, Mandal SK. Rational drug design. *Eur. J. Pharmacol*. 2009;625(1-3):90-100. [DOI: 10.1016/j.ejphar.2009.06.065]

Mehta H, Khokra SL, Arora K, Kaushik P. Pharmacophore mapping and 3D-QSAR analysis of *Staphylococcus aureus* Sortase a inhibitors. *Der Pharm. Chem.* 2012;4(5): 1776-84.

Park Choo H-Y, Choi S, Jung S-H, Koh HY, Pae AN. The 3D-QSAR study of antitumor arylsulfonylimidazolidinone derivatives by CoMFA and CoMSIA. *Bioorg. Med. Chem*. 2003;11(21):4585-9. [DOI: 10.1016/S0968-0896(03)00530-3]

Phase, version 3.6, Schrodinger, LLC, New York, 2013.

Rathi Suganya P, Kalva S, Saleena LM. Pharmacophore modeling, atom based 3D-QSAR and docking studies on ADAMTS-5 inhibitors. *IPCBEE* 2011;5:378-82.

Saliner AG, Girones X. Topological quantum similarity measures: applications in QSAR. *J. Mol. Str.: Theochem*. 2005;727(1-3):97-106. [DOI: 10.1016/j.theochem.2004.11.062]

Seidel T, Ibis G, Bendix F, Wolber G. Strategies for 3D pharmacophore-based virtual screening. *Drug Discov. Today: Technol.* 2010;7(4):e221-8. [DOI: 10.1016/j.ddtec.2010.11.004]

Sharma V, Wakode SR, Lather V, Mathur R, Fernandes MX. Structure based rational drug design of selective phosphodiesterase-4 ligands as anti-inflammatory molecules. *Bull. Pharm. Res.* 2011; 1(2):33-40.

Tang Y, Zhu W, Chen K, Jiang H. New technologies in computer-aided drug design: Toward target identification and new chemical entity discovery. *Drug Discov. Today Technol*. 2006;3(3):307-13.

*****